Carlson, K.D., and Beckermann, C., "Use of the Niyama Criterion to Predict Shrinkage-Related Leaks in High-Nickel Steel and Nickel-Based Alloy Castings," in Proceedings of the 62nd SFSA Technical and Operating Conference, Paper No. 5.6, Steel Founders' Society of America, Chicago, IL, 2008.

Use of the Niyama Criterion To Predict Shrinkage-Related Leaks in High-Nickel Steel and Nickel-Based Alloy Castings

Kent D. Carlson and Christoph Beckermann

Department of Mechanical and Industrial Engineering

The University of Iowa, Iowa City, IA 52242

Abstract

A common simulation output variable routinely used by foundries to detect solidification shrinkage defects in steel castings is the Niyama criterion (*Ny*), which is defined as the local thermal gradient divided by the square root of the local cooling rate. For sufficiently large Niyama values, no shrinkage porosity forms. When the Niyama value decreases below a critical value, Ny_{micro}, small amounts of micro-shrinkage begin to form. As the Niyama value decreases further, the amount of micro-shrinkage increases until it becomes detectable on a standard radiograph. This transition occurs at a second critical value, Ny_{macro}. The amount of shrinkage porosity continues to increase as the Niyama criterion decreases below Ny_{macro}. A previous study by the present authors determined that Ny_{macro} = 1.0 (°C-s)$^{1/2}$/mm for nickel-based alloys M30C, M35-1 and CW12MW, and for austenitic stainless steel type CN7M. The purpose of the present study is to develop a tool to predict micro-shrinkage in high-nickel alloys by determining Ny_{micro}. This is accomplished by performing metallographic analyses on two case study castings (a CN7M valve and a M35-1 valve) in which leakage occurred. In both cases the pouring and solidification of these castings was simulated, and careful comparisons were made to correlate the resulting Niyama criterion values to regions containing micro-porosity (and macro-porosity). The results indicate that the Niyama criterion is capable of predicting the probability of leakage due to interconnected macro- and/or micro-shrinkage porosity. The case studies indicate that macro-shrinkage (visible on a radiograph) may be present in casting regions with $Ny < Ny_{macro}$ = 1.0 (°C-s)$^{1/2}$/mm, which validates previous research. More importantly, these case studies indicate that noticeable amounts of micro-shrinkage may be present in casting regions with $Ny < Ny_{micro}$ = 2.0 (C-s)$^{1/2}$/mm. These results imply that leaks in high-nickel alloy castings can be prevented by ensuring that simulated Niyama values are above 2.0 (C-s)$^{1/2}$/mm. This does not, however, imply that one should attempt to keep $Ny > 2.0$ (C-s)$^{1/2}$/mm throughout the casting. While that may be possible, it may be impractical and expensive to ensure such a high level of soundness throughout the casting. For the purpose of preventing leaks, it is only necessary to ensure that there not be a potential "pathway" of shrinkage porosity (micro- and/or macro-porosity) that leads from the inside to the outside of a fluid-containing casting.

Introduction

Leaks in fluid-containing castings (e.g., valves, pumps, etc.) are a major cause of unscheduled and costly shutdowns for users and a lesser cause of casting rejections at the foundry or equipment manufacturer. Such leaks may be caused by macro-shrinkage (visible solidification shrinkage, which may be detected by common radiographic techniques), micro-shrinkage (solidification shrinkage that is not visible on a standard radiographic film), other casting features, or some combination of these causes. If a leak is the result of macro-shrinkage, it may be detected by radiography. In this case, the shrinkage causing the leak is frequently eliminated through the use of additional risers and/or chills. Such procedures lower the casting yield and increase rigging cost. Industry standards for radiography produce radiographs with 2% sensitivity. This implies, for example, that for a defect to be detectable on a radiograph of a 2.54 cm (1 in) thick section, the defect must correspond to a lost-section thickness of at least 0.5 mm (0.020 in). Smaller shrinkage will not be detected via radiography. If a leak is caused by such micro-shrinkage, it is often only detected after machining operations or during pressure testing. In the worst case, a micro-shrinkage-related leak may not be detected until after the casting has been placed in service, increasing costs to both the foundry and the end user. Present risering rules are primarily intended to prevent macro-shrinkage detectable by radiographic testing; little is known about proper risering procedures to prevent micro-shrinkage. A review of risering rules for steel castings is given in Carlson *et al*.[1]

Over the course of about the past quarter-century, foundries have begun to rely increasingly upon casting simulation software to predict and improve casting quality. A common simulation output variable routinely used by foundries to detect solidification shrinkage defects in steel castings is known as the Niyama criterion[2]. The Niyama criterion is defined as the local thermal gradient divided by the square root of the local cooling rate (i.e., $Ny = G/\sqrt{\dot{T}}$). Common units for the Niyama criterion are $(\text{C-s})^{1/2}/\text{mm}$, $(\text{C-min})^{1/2}/\text{cm}$ and $(\text{F-min})^{1/2}/\text{in}$; the relationship between these units is 1.0 $(\text{C-s})^{1/2}/\text{mm}$ = 1.29 $(\text{C-min})^{1/2}/\text{cm}$ = 4.40 $(\text{F-min})^{1/2}/\text{in}$. The Niyama criterion is evaluated near the end of solidification, when solidification shrinkage forms. In the present study, the Niyama values are evaluated at a temperature 10% of the solidification range above the 100% solid (i.e., solidus) temperature; i.e., $T_{Ny} = T_{sol} + 0.1\left(T_{liq} - T_{sol}\right)$. This is important to note, as the choice of Niyama evaluation temperature can significantly influence the resulting Niyama values[3].

The relationship between shrinkage porosity and the Niyama criterion is shown schematically in Fig. 1. For sufficiently large Niyama values, no shrinkage porosity forms. When the Niyama value decreases below a critical value, Ny_{micro}, small amounts of micro-shrinkage begin to form. As the Niyama value decreases further (note the log scale on the x-axis), the amount of micro-shrinkage increases until it becomes detectable on a standard radiograph. This transition occurs at a second critical value, Ny_{macro}. The amount of shrinkage porosity continues to increase as the Niyama criterion decreases below Ny_{macro}. It should be emphasized that the Niyama criterion only predicts feeding-distance related shrinkage; it does not explicitly predict hot spots in a casting, and it does not predict gas porosity.

A previous study by the present authors[4] determined the value of Ny_{macro} for nickel-based alloys M30C, M35-1 and CW12MW, and for austenitic stainless steel type CN7M, using a

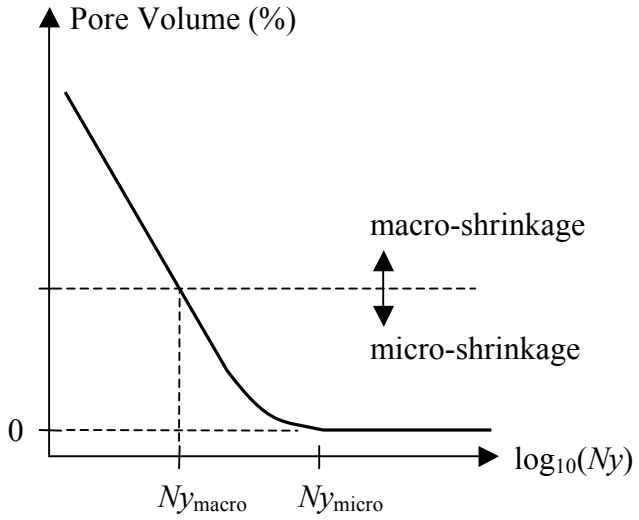

Fig. 1 Schematic illustrating the relationship between shrinkage porosity volume and the Niyama criterion.

combination of casting experiments and simulation. For these four high-nickel alloys, end-risered plates with a thickness of 2.54 cm (1 in) were cast in a variety of lengths, to produce levels of casting soundness ranging from very sound to extremely unsound (i.e., extensive centerline shrinkage). All of these plates were then radiographed. The casting of these plates was simulated using recorded casting data, and the simulated Niyama values were compared to the plate radiographs. A sample comparison is shown for a CN7M plate in Fig. 2. Note the correlation between visible shrinkage porosity in the radiograph and low Niyama values (blue regions) in the simulation results. Based on these comparisons, it was determined that the critical Niyama value for macro-shrinkage for these high-nickel alloys is $Ny_{macro} = 1.0$ (C-s)$^{1/2}$/mm.

Casting leaks caused by macro-porosity can be detected with radiography, and they can be predicted using the Niyama criterion as described above. However, leaks caused by micro-porosity cannot be detected by either of these methods. The purpose of the present study is to develop a tool to predict micro-shrinkage in high-nickel alloys by determining Ny_{micro}, as depicted in Fig. 1. This is accomplished by performing metallographic analyses on two case study castings in which leakage occurred, simulating the pouring and solidification of these castings[1], and making careful comparisons to correlate the resulting Niyama criterion values to regions containing micro-porosity (and macro-porosity).

[1] The simulations performed for this study were conducted using the casting simulation software package MAGMASOFT[5]. A wide variety of simulation packages are commercially available, and most of them calculate the Niyama criterion. A recent round-robin study conducted by the present authors[3] directly compared Niyama results generated with different simulation packages.

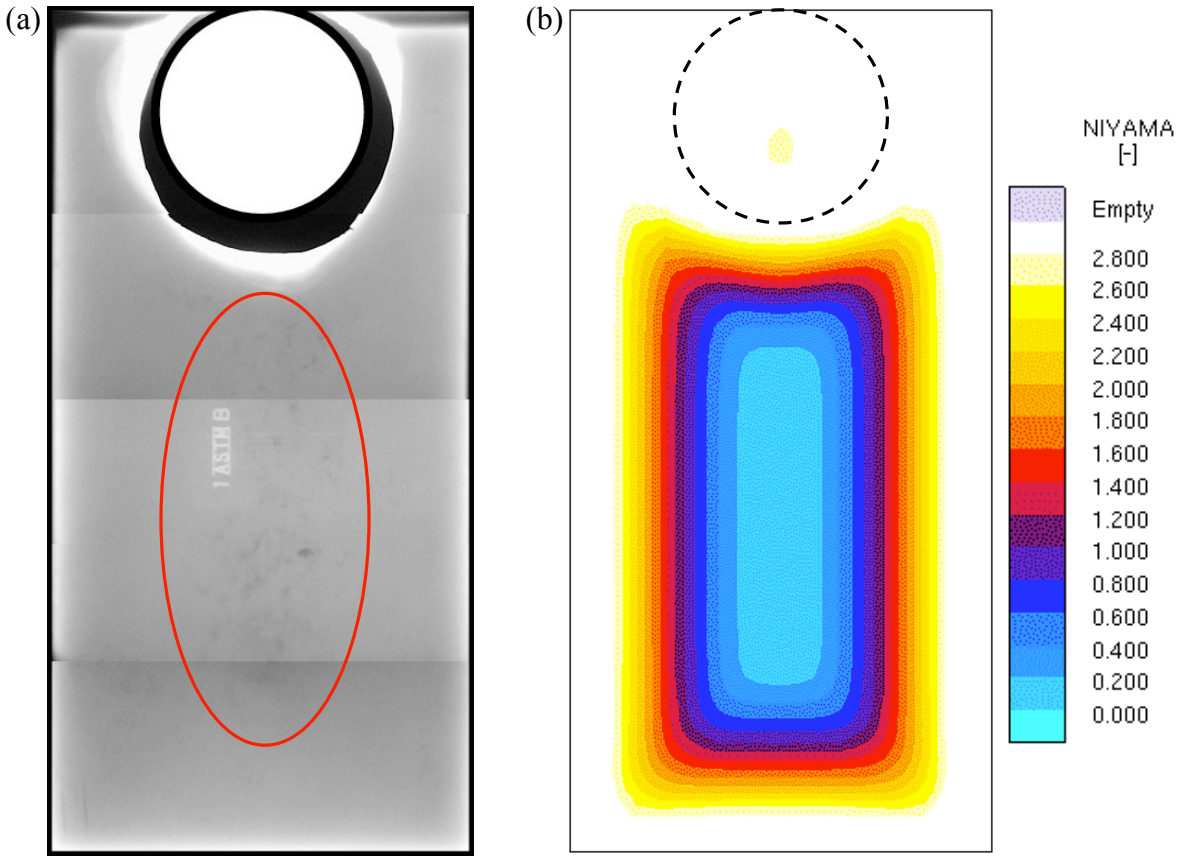

Fig. 2 Comparison between (a) experimental and (b) simulated results for a 1”T x 8”W x 16”L (2.54 x 20.3 x 40.6 cm) CN7M plate casting with a 4” (10.2 cm) diameter riser. The radiograph in (a) was rated x-ray level 3; the red circle denotes the region of the radiograph with visible shrinkage. The Niyama contours shown in (b) are taken at the plate mid-plane.

Case Study 1

The first case study is an investment cast alloy M35-1 valve. Eight valves, all the same model and poured from the same heat, were shipped from the foundry to a customer. One of these eight valves leaked during the customer’s pressure test, and was returned to the foundry. Photographs of this valve are shown in Fig. 3. The inner diameter (ID) and outer diameter (OD) sides of the leak are indicated in Fig. 3b. When the foundry recovered the valve, a section containing the leak was cut from the valve for metallographic analysis. The location of this section is indicated by interrupted lines in Fig. 3b. Photographs of the OD of the extracted section containing the leak are provided in Fig. 4. These photographs show that the leak exit appears to be macro-shrinkage, and that the exit location is about 1 mm (0.039 in) from the valve mid-plane. In addition to obtaining a metallographic analysis of the leaking section, the present researchers also obtained metallographic analyses of five additional regions. The location of the leaking region and the

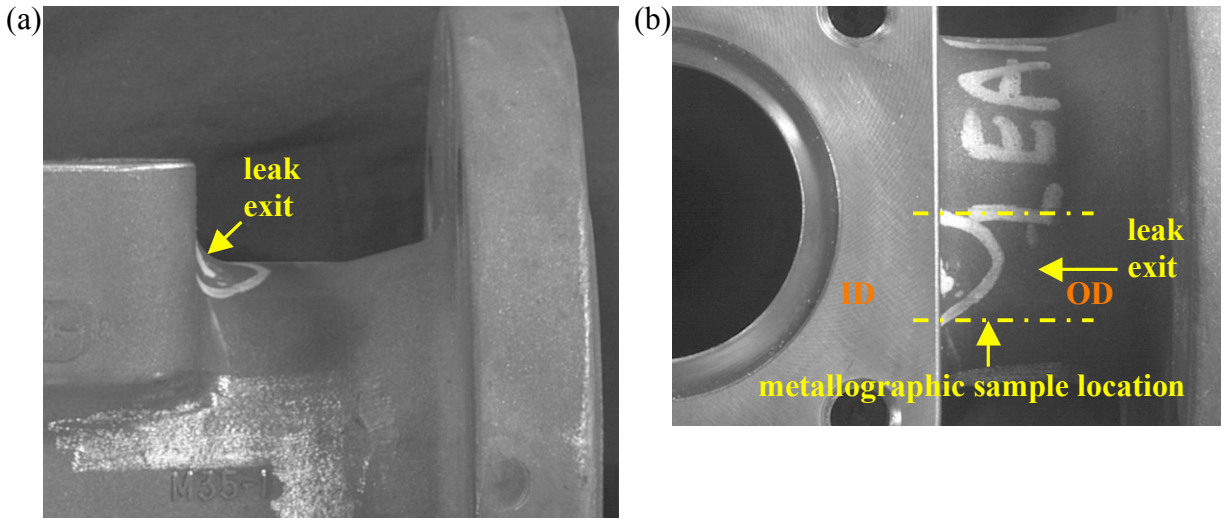

Fig. 3 Photographs of the M35-1 valve, indicating the leak exit location: (a) valve side view; and (b) valve bottom view, showing the leak exit location and indicating with dashed lines the size of the sample cut from the valve to analyze the leaking section.

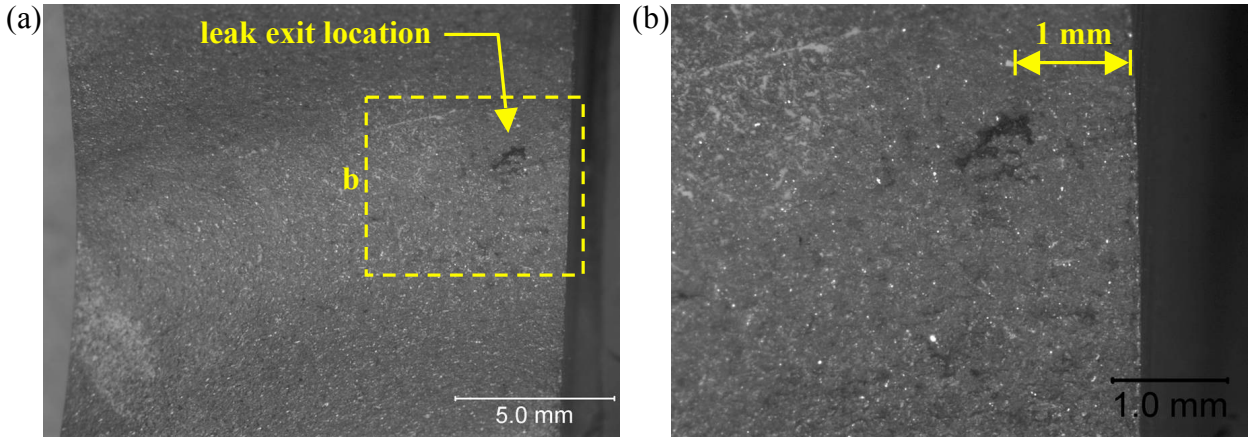

Fig. 4 Photographs of the OD surface of the section containing the leak that was cut from the valve: (a) a view of the entire thickness of the cut section; and (b) a close-up of the leak exit location. The dashed rectangle in (a) indicates the area shown in (b). The vertical surface on the right of these photographs corresponds to the valve mid-plane.

five additional regions are indicated in Fig. 5, which is a photograph of the valve sectioned at the mid-plane.

The investment casting process for this valve was simulated using casting data that was supplied by the foundry. For the simulation, the valve and gating assembly (not shown for proprietary reasons) was coated with a 10 mm (0.39 in) thick shell coating using a shell generation option in the casting simulation software. The pouring temperature for the simulation was taken as 1450 C (2642 F), and the pouring time was 7 s. The initial temperature of the shell

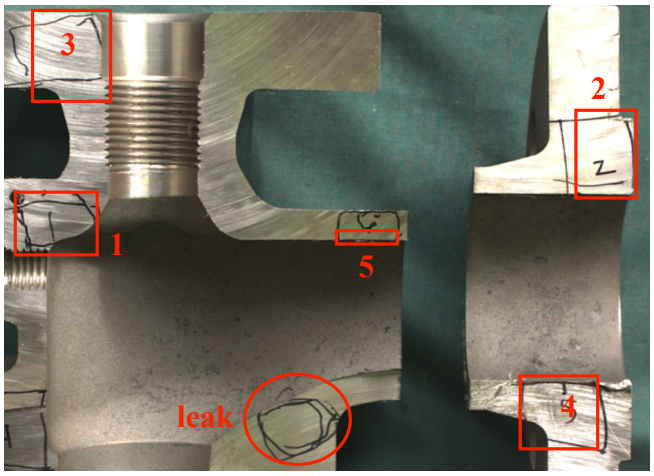

Fig. 5 Photograph of the valve after being sectioned at the mid-plane, indicating the location of the leak as well as the five additional regions where metallographic examination was performed.

in the simulation was set to 800 C (1472 F), to account for the shell preheat provided by the foundry. The alloy was modeled using a M35-1 material database developed by the present researchers[4]. According to the foundry, their shell was primarily fused silica sand. Two sand mold databases provided with the casting simulation software were considered to model this shell: a database for dry silica sand and a database called 'shell sand'. Simulations were run using both of these sand databases; the Niyama values in the regions of interest were slightly lower (up to about 0.2 $(C\text{-}s)^{1/2}$/mm lower) with the dry silica sand database than with the shell sand database, so the dry silica sand database was selected because it provided the more conservative estimate of the two databases. The insulating sleeve around the pouring cup was modeled with properties supplied by the sleeve manufacturer. The interfacial heat transfer coefficient (HTC) between the metal and the shell was taken as a constant value of 1000 W/m^2-K (176 Btu/h-ft^2-F). This value is very approximate; however, simulations were run varying the HTC by a factor of two, and the difference in the resulting Niyama criterion values was negligible. The HTCs between the insulating sleeve and the other components were taken from HTC datasets supplied by the sleeve manufacturer. The simulation used a grid containing about 791,000 metal cells. It should be noted that there may be some inaccuracies in this investment casting simulation, due to uncertainties in parameters such as the shell sand material properties and the interfacial shell/metal heat transfer coefficient (as discussed above). Also, radiation effects on the exterior surface of the shell are only approximately accounted for in the simulation. However, parametric studies such as the ones described above indicate that the resulting Niyama contours are relatively insensitive to these quantities.

A comparison between experimental results and Niyama criterion contours at the valve mid-plane in the vicinity of the leak (see Fig. 5) is given in Fig. 6. The rectangles with letters beside them in this figure (and subsequent figures) indicate areas represented in the photographs corresponding to that letter. Fig. 6a shows the dendritic nature of the features, confirming that they are indeed shrinkage. Fig. 6b shows visible shrinkage porosity in the area of the ID of the leak. The region showing considerable shrinkage in Fig. 6b corresponds to a region with $Ny <$ 1.0 $(C\text{-}s)^{1/2}$/mm in Fig. 6c. The minimum Niyama value along the ID surface in Fig. 6c is 0.6 (C-

s)$^{1/2}$/mm, and the minimum value at the OD surface is 0.5 (C-s)$^{1/2}$/mm. The macro-shrinkage seen at the ID in Fig. 6b and at the OD in Fig. 4 corroborate the findings in previous work[4] by the present authors that indicate that macro-shrinkage in M35-1 is likely to occur in regions where $Ny < 1.0$ (C-s)$^{1/2}$/mm.

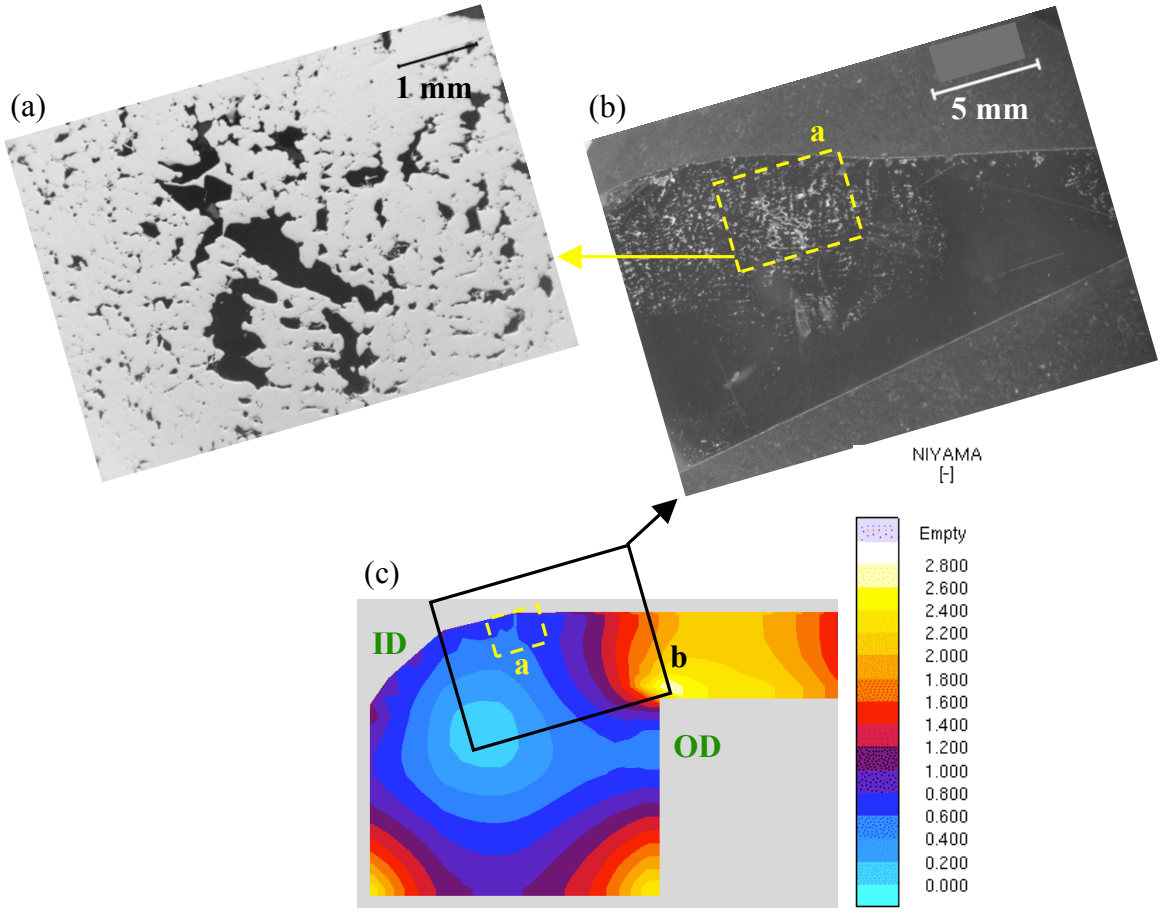

Fig. 6 Comparison between photographs of the valve mid-plane surface at the leak location and simulation results at the same location: (a) and (b) are photographs of shrinkage porosity near the ID surface; and (c) is a Niyama contour plot of the region. The rectangles indicate areas represented by photographs; letters next to each rectangle indicate which photograph that area represents.

Analogous comparisons between experimental results and Niyama criterion contours at the valve mid-plane are given in Fig. 7 to Fig. 11 for the five regions indicated by rectangles in Fig. 5. The photographs of Region #1 shown in Fig. 7 indicate that there is only a small amount of shrinkage porosity in this region. The Niyama values in Fig. 7c corresponding to the area shown in Fig. 7a are mostly in the range $1.6 < Ny < 2.1$ (C-s)$^{1/2}$/mm. There are some low Niyama values (i.e., blue contours) in Fig. 7c, in the lower left of the rectangle representing the area shown in Fig. 7b, but they correspond to a region of the valve that had a threaded hole machined into it (the threads are visible in the lower left of Fig. 7b). Most of the area represented in Fig. 7b has Niyama values greater than 1.0. Region #2 is depicted in Fig. 8. The photographs in Fig. 8a to Fig. 8c show some micro-shrinkage throughout much of this region. The holes visible near the

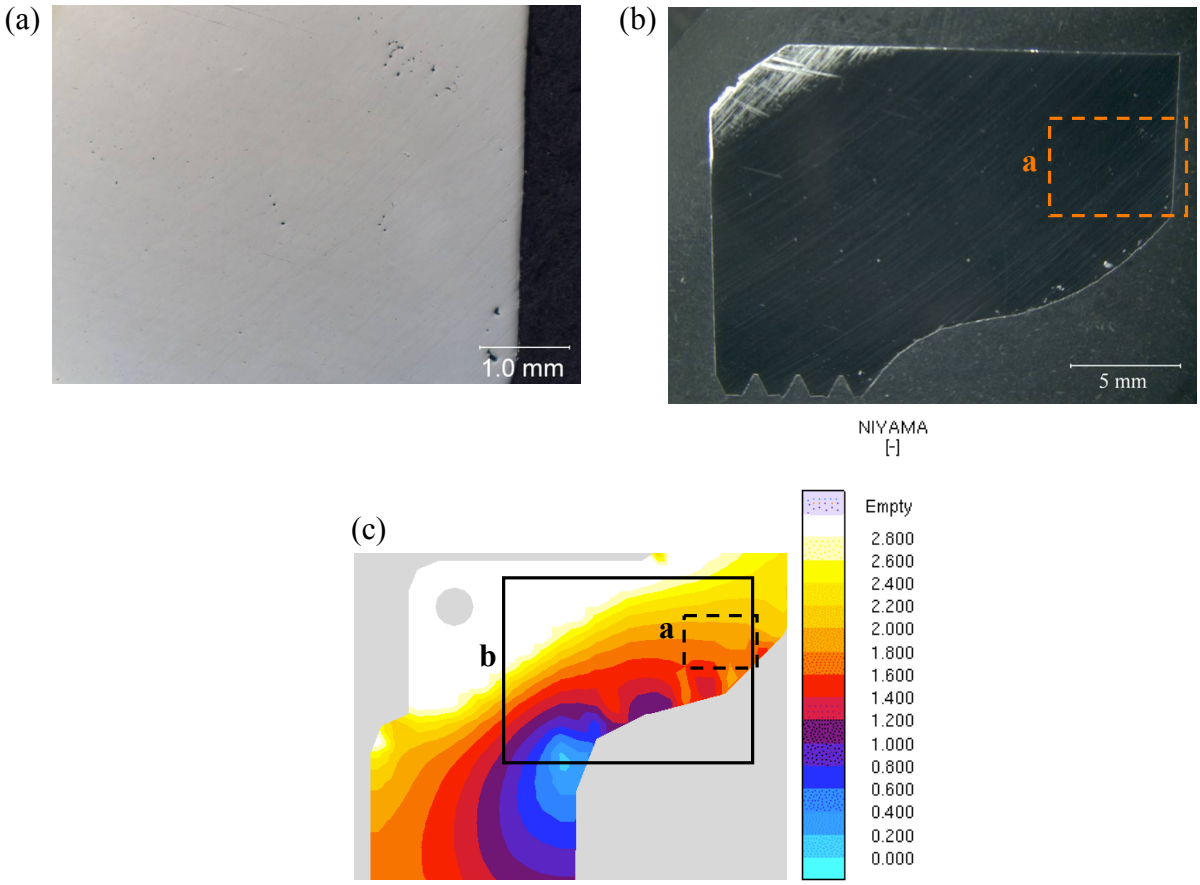

Fig. 7 Comparison between photographs of the valve mid-plane surface at Region #1 and simulation results at the same location: (a) and (b) are photographs of Region #1; and (c) is a Niyama contour plot of the region. The rectangles indicate areas represented by photographs; letters next to each rectangle indicate which photograph that area represents.

valve surface in Fig. 8a are likely not shrinkage porosity; such near-surface defects will be seen in several of these regions. Fig. 8d provides the simulated Niyama contours for this region. Note that the Niyama values are lower in the area corresponding to Fig. 8b ($1.3 < Ny < 1.5$ (C-s)$^{1/2}$/mm) than in the area corresponding to Fig. 8a ($1.2 < Ny < 2.6$ (C-s)$^{1/2}$/mm), and that more micro-shrinkage is seen in Fig. 8b than in Fig. 8a. The comparison for the upper portion of Fig. 8a is approximate, because the simulation of the valve approximates the corner contained in Fig. 8a as a right angle, rather than rounding it with a fillet as seen in Fig. 8a. The comparison for Region #3 is shown in Fig. 9. Fig. 9a to Fig. 9c show shrinkage porosity throughout the region. The larger circles seen in Fig. 9c are water spots. The right surface in Fig. 9c was machined after casting, so that surface does not quite correspond to the simulation result shown in Fig. 9d. Relatively low Niyama values ($Ny < 1.6$ (C-s)$^{1/2}$/mm) persist throughout this region, and shrinkage porosity is evident in most of this region. A nice correlation between the Niyama criterion and shrinkage is seen in Fig. 9a, where the significant shrinkage in the upper left corner decreases moving toward the lower right, and the Niyama value increases in the same direction. The pale purple region seen in the upper right of Fig. 9d indicates that those computational cells

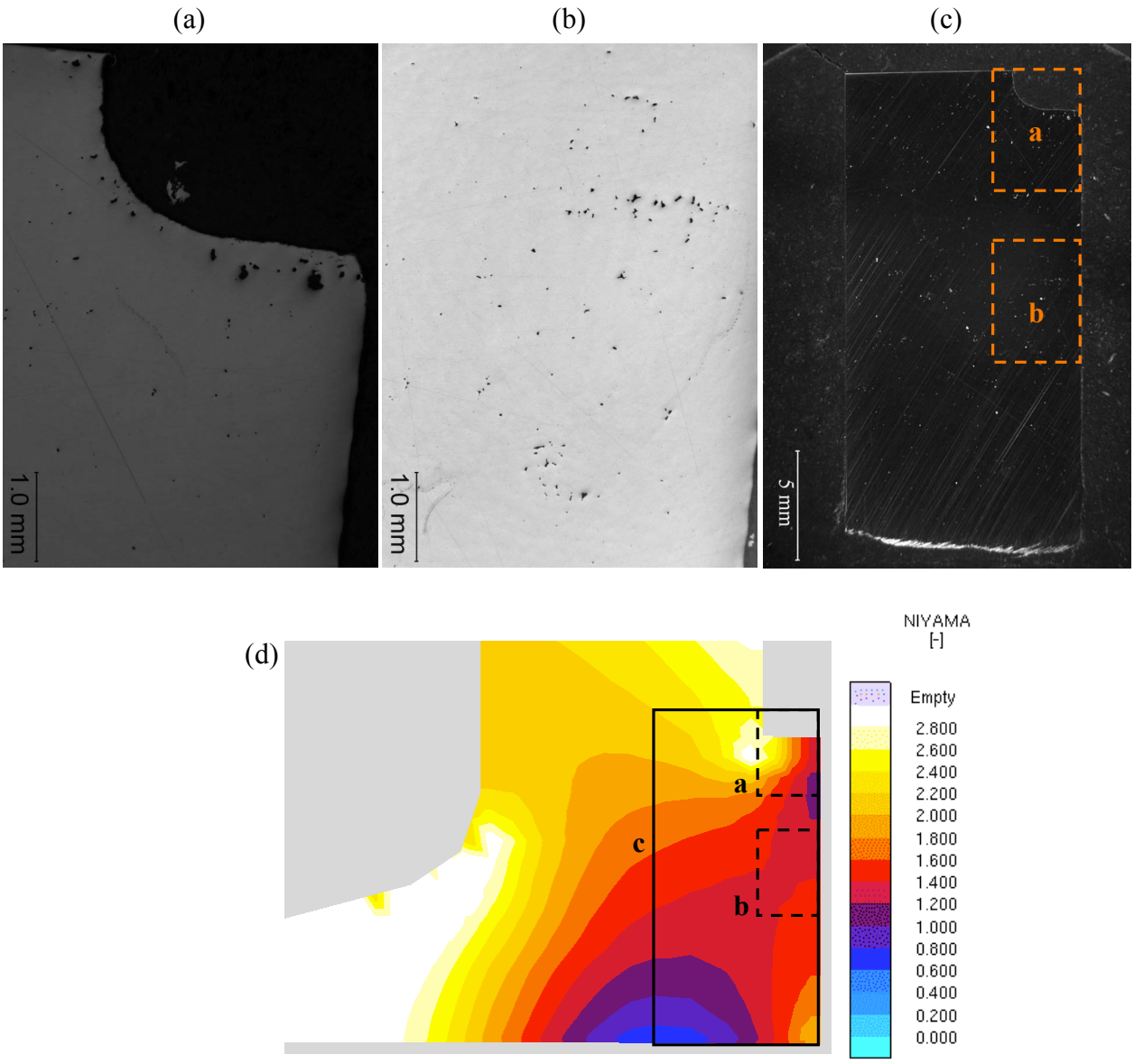

Fig. 8 Comparison between photographs of the valve mid-plane surface at Region #2 and simulation results at the same location: (a) - (c) are photographs of Region #2; and (d) is a Niyama contour plot of the region. The rectangles indicate areas represented by photographs; letters next to each rectangle indicate which photograph that area represents.

are empty because metal drained down during solidification (as in a riser pipe). The photograph in Fig. 9c indicates that there is significant shrinkage in this region, but it is not empty of metal. This indicates that the simulation is not quite accurate near this surface. Region #4 is depicted in Fig. 10. A significant amount of shrinkage porosity is evident in Fig. 10a to Fig. 10e, and Fig. 10f indicates that most of this region has $Ny < 1.0$ $(\text{C-s})^{1/2}/\text{mm}$. In Fig. 10d, a smaller amount of shrinkage is seen near the bottom of the sample, where $1.0 < Ny < 1.6$ $(\text{C-s})^{1/2}/\text{mm}$. Again, Fig. 10c and Fig. 10d show holes that are likely non-shrinkage defects near the casting surface.

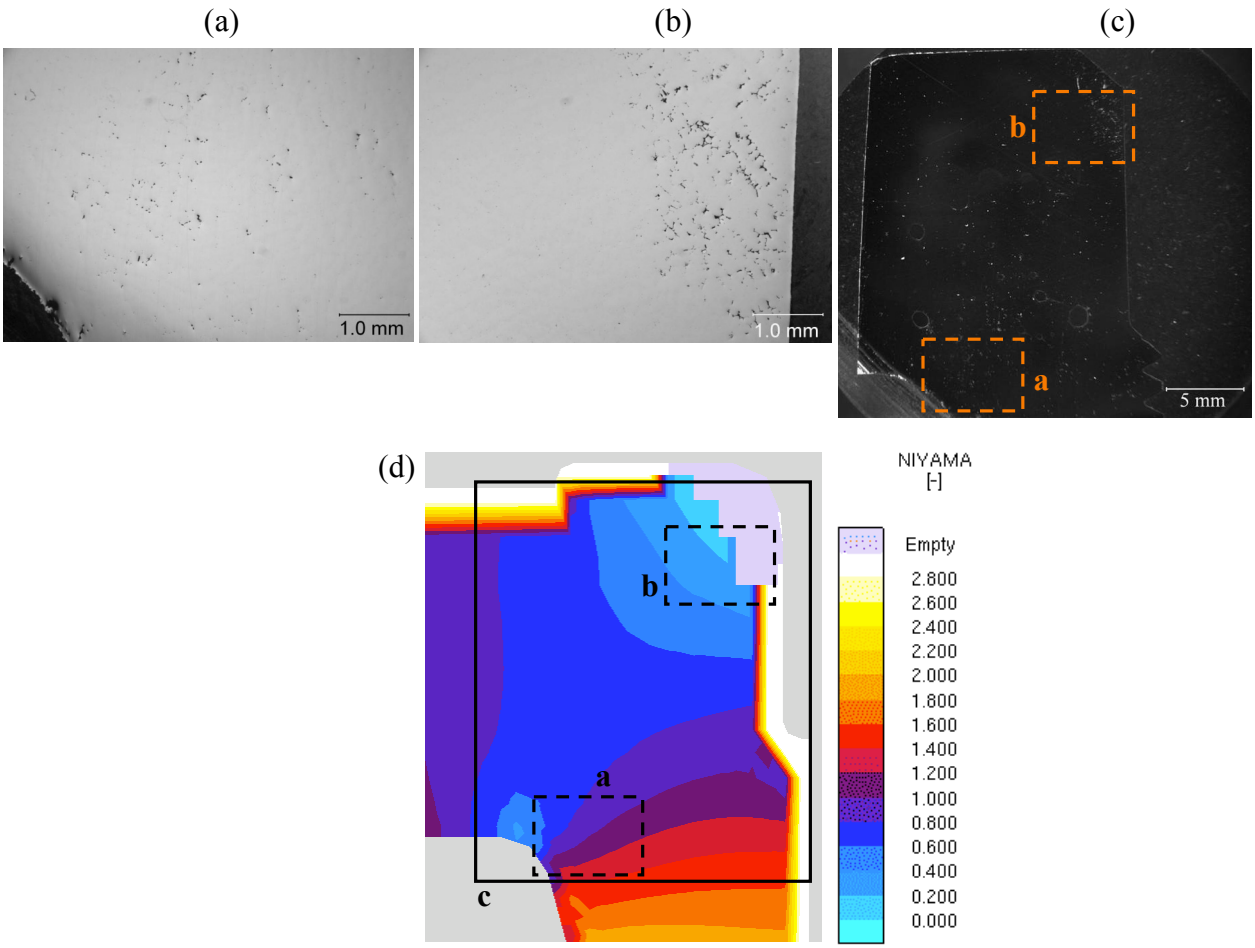

Fig. 9 Comparison between photographs of the valve mid-plane surface at Region #3 and simulation results at the same location: (a) - (c) are photographs of Region #3; and (d) is a Niyama contour plot of the region. The rectangles indicate areas represented by photographs; letters next to each rectangle indicate which photograph that area represents.

Finally, Fig. 11 depicts Region #5. The photograph in Fig. 11a shows about 3 mm (0.118 in) of a wall region, starting at the ID. This region shows a significant amount of shrinkage porosity. The Niyama values seen in Fig. 11b reflect this, with values less than 1.0 $(C\text{-}s)^{1/2}$/mm throughout the area seen in Fig. 11a.

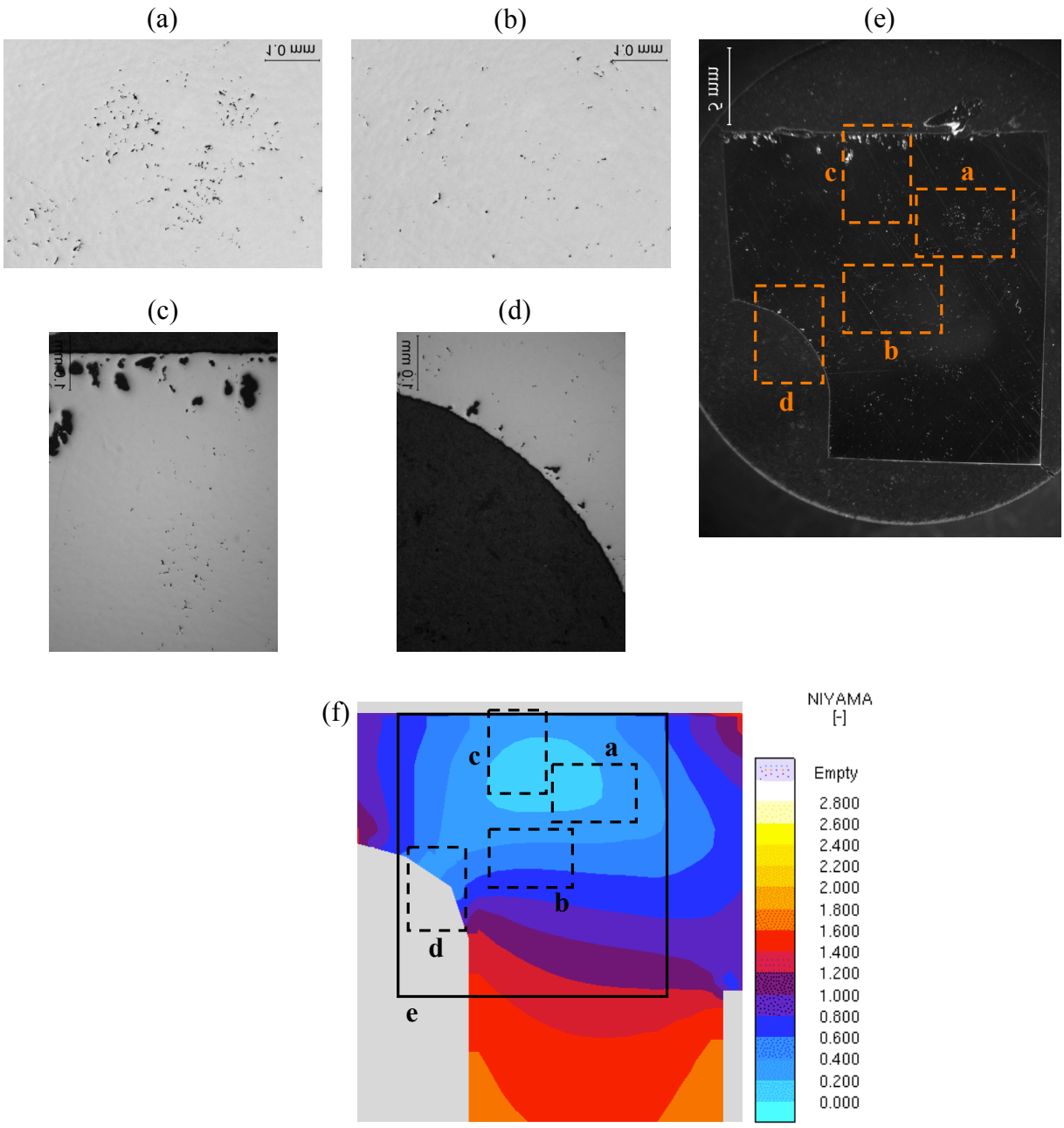

Fig. 10 Comparison between photographs of the valve mid-plane surface at Region #4 and simulation results at the same location: (a) - (e) are photographs of Region #4; and (f) is a Niyama contour plot of the region. The rectangles indicate areas represented by photographs; letters next to each rectangle indicate which photograph that area represents.

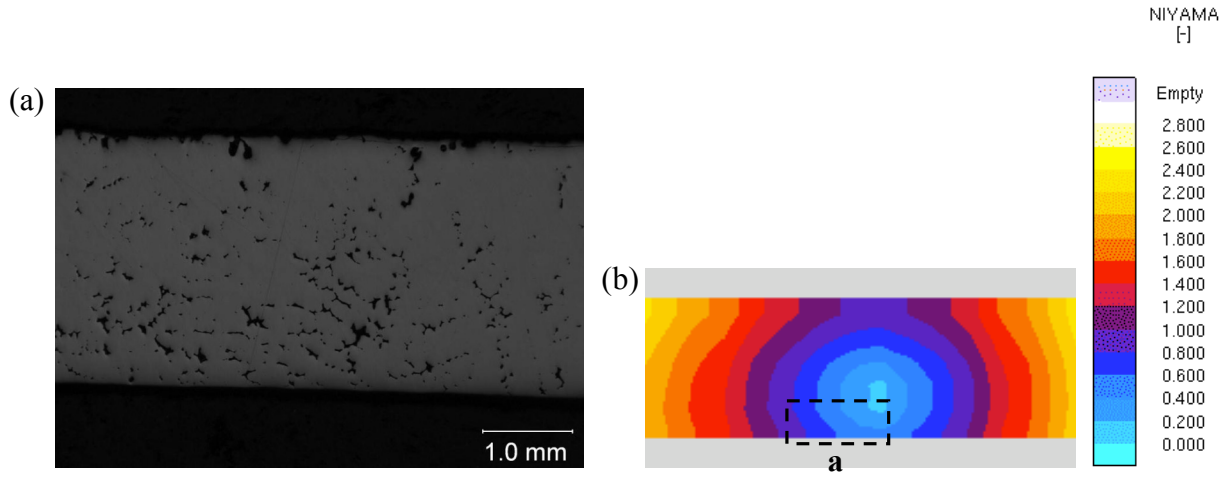

Fig. 11 Comparison between a photograph of the valve mid-plane surface at Region #5 and simulation results at the same location: (a) is a photograph of Region #5; and (b) is a Niyama contour plot of the region. The rectangle indicates the area represented by the photograph.

In summary, comparisons between experimental results and Niyama values for the regions of the M35-1 valve investigated in this case study indicate that the Niyama criterion does indeed seem to correlate with both macro- and micro-shrinkage porosity. In general, regions with $Ny <$ 1.0 $(\text{C-s})^{1/2}$/mm show a significant amount of shrinkage porosity (macro-porosity). Regions with $1.0 < Ny <$ 2.0 $(\text{C-s})^{1/2}$/mm often show a noticeable amount of micro-shrinkage, and regions with $Ny >$ 2.0 $(\text{C-s})^{1/2}$/mm show very little or no shrinkage porosity.

Case Study 2

The second case study is an austenitic stainless steel type CN7M valve casting. A leak occurred in two different valves that were in hydrofluoric acid (HF) service. Both valves, which were the same model but were cast from different heats, leaked within the first week of service. Fig. 12 shows photographs of one of these valves that illustrate the leak exit location. This valve was then sectioned, and photographs were taken of the inside of the valve section containing the leak. These photographs are shown in Fig. 13. The section of the valve containing the leak was then radiographed. Digitized radiographs of this valve section are shown in Fig. 14, demonstrating visible shrinkage porosity in the region of the leak. Finally, the valve section containing the leak was cut directly through the leaking region. This cut surface was then etched and photographed, as shown in Fig. 15. These photographs clearly show a void and interconnected macro-shrinkage in the center of the leaking wall, with smaller amounts of shrinkage extending toward the inner diameter (ID) and outer diameter (OD) surfaces. No visible porosity reaches the OD surface of the section shown. The second leaking valve leaked in the same general area as did the first, a little bit closer to the flange (i.e., the leak exit was a little bit above the location indicated in Fig. 12a). Because the leak location is similar and the leak was also determined to be the result of shrinkage porosity, photographs of the second are not included here. Once these leaking valves were discovered, the casting foundry revised their rigging for this valve. No further leaks have been reported since the rigging was revised.

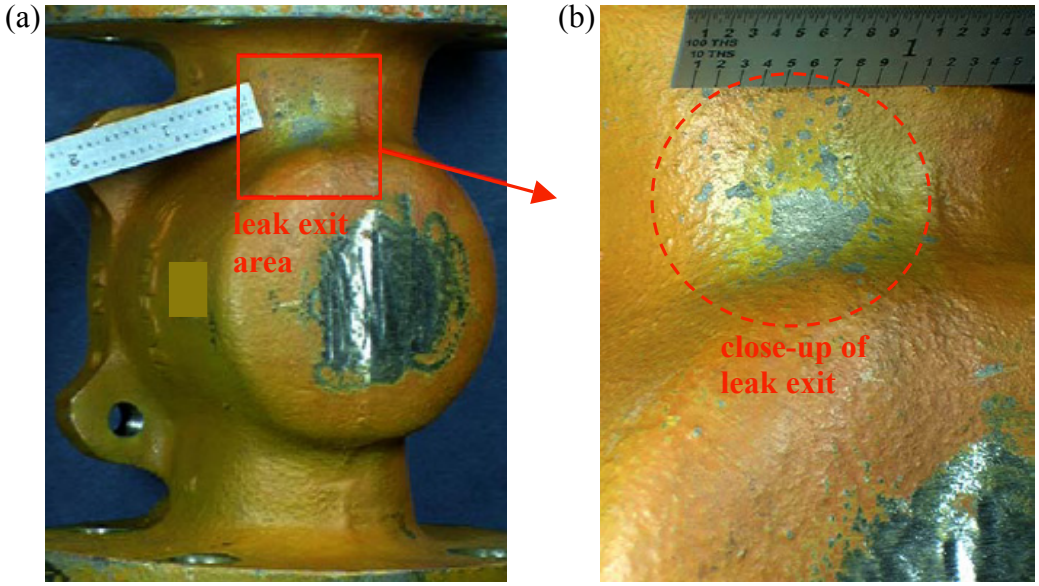

Fig. 12 Photographs of a leaking CN7M valve, showing the exit location of the leak: (a) valve view showing full leak exit location; and (b) a close-up of leak exit location.

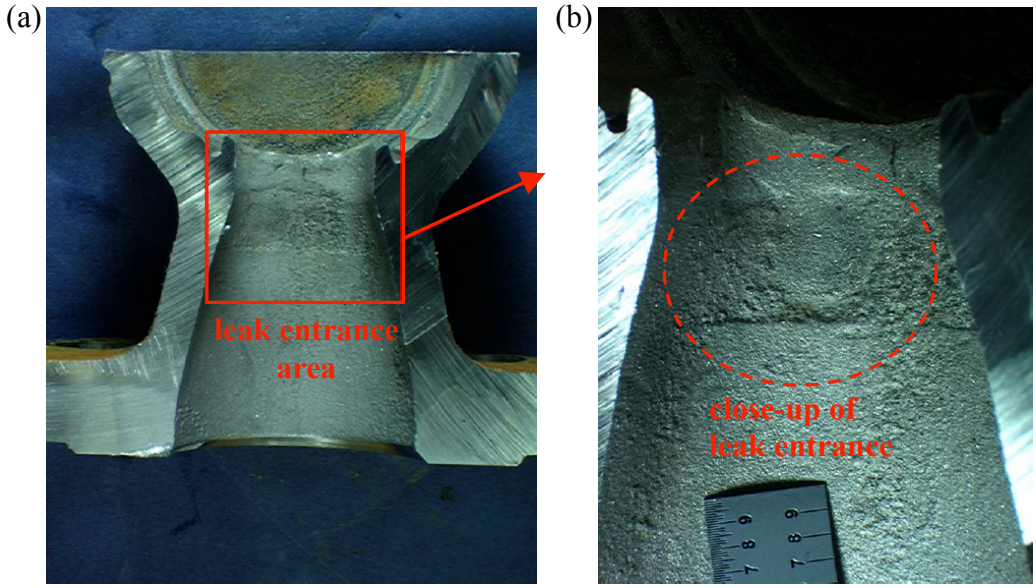

Fig. 13 Photographs showing the entrance location of the leak: (a) view of valve section containing leak; and (b) a close-up of leak entrance location.

The casting of this valve was simulated, both with the original rigging and with the revised rigging. Both simulations were performed using the following casting data, which was supplied by the foundry. The pouring temperature was 1520 C (2768 F), and pouring was dependent on an inlet pressure profile developed by the foundry. The alloy was modeled using a CN7M material database developed by the present researchers[4]. The sand mold was modeled with chemically bonded urethane molding sand properties, and the core material was modeled with chemically

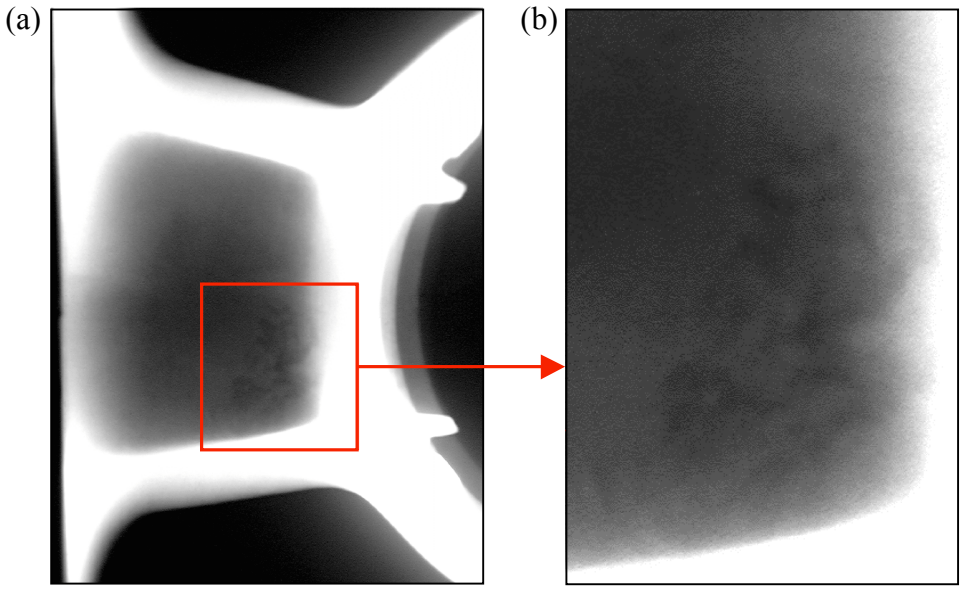

Fig. 14 Digitized radiograph showing visible shrinkage porosity in the region of the leak: (a) view of the valve section containing the leak (same view as shown in Fig. 13b); and (b) a close-up of the shrinkage porosity.

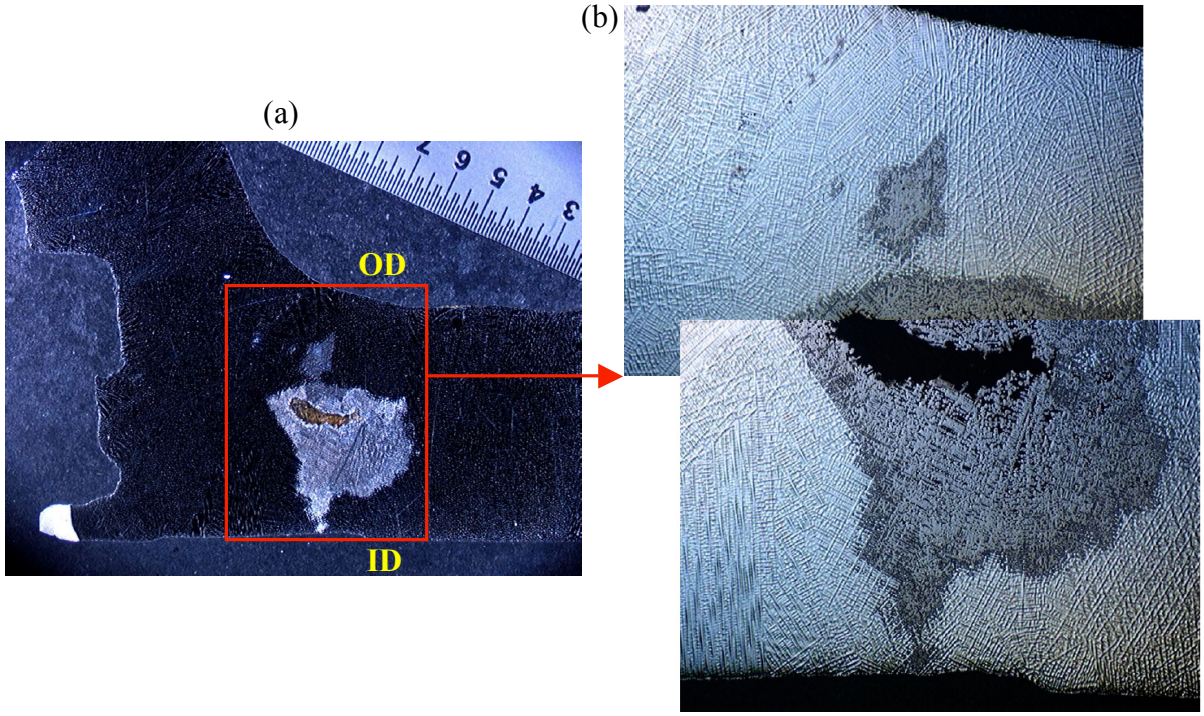

Fig. 15 Photographs of an etched cross-section through the leaking region: (a) view of the valve wall containing the leak; and (b) a close-up view of the visible shrinkage porosity.

bonded shell molding sand properties. Both of these sand property datasets were supplied by the foundry, who noted that the data was taken from reference [6]. The chills were modeled with steel properties supplied by the foundry, and the riser sleeves were modeled with properties supplied by the manufacturer. All interfacial heat transfer coefficients (HTCs) were taken as constant values, supplied by the foundry. The sand-metal HTC was 1000 W/m^2-K (176 Btu/h-ft^2-F), the sand-chill HTC was 1500 W/m^2-K (264 Btu/h-ft^2-F), and the metal-chill HTC was 2000 W/m^2-K (352 Btu/h-ft^2-F). The HTCs between the riser sleeves and the other components were taken from HTC datasets supplied by the sleeve manufacturer. Finally, the simulation with the original rigging used a grid containing about 741,000 metal cells, while the simulation with the revised rigging used a grid containing about 935,000 metal cells.

A plot of the Niyama criterion contours at the valve mid-plane for the simulation with the original rigging is provided in Fig. 16. This plot shows an area of low Niyama values in the leaking region. Note the symmetry on either side of the valve body in this contour plot, which is the result of the relative thermal symmetry of the rigging. Fig. 17b provides a close-up valve mid-plane view of the original rigging Niyama results in the leaking region. The photograph of the etched cross-section of the leaking region from Fig. 15a is repeated for comparison in Fig. 17a. Note that the visible macro-shrinkage extending outward from this void corresponds well with the region of low Niyama values (the light blue regions) in Fig. 17b. This agrees with findings in previous work[4] by the present authors, indicating that macro-shrinkage in CN7M is likely to occur in regions where $Ny < 1.0$ (C-s)$^{1/2}$/mm. In Fig. 17b, the minimum Niyama value at the ID surface is 0.6 (C-s)$^{1/2}$/mm, and the minimum value at the OD surface is 1.7 (C-s)$^{1/2}$/mm. The minimum Niyama values at the ID and OD surfaces do not change significantly in the neighborhood of the valve mid-plane; the minimum Niyama values found within ± 5 mm (±0.20 in) of the valve mid-plane at both the ID and OD surfaces are at most 0.1 (C-s)$^{1/2}$/mm lower than the minimum values at the mid-plane. Taking the smallest OD surface Niyama value in the neighborhood of the valve mid-plane, this simulation indicates that micro-shrinkage sufficient to cause leaks can exist at Niyama values of about 1.6 (C-s)$^{1/2}$/mm.

The Niyama criterion contour plot for the revised rigging is given in Fig. 18. Comparison between this plot and Fig. 16 indicates that the Niyama values have significantly increased in the region that leaked with the original rigging. Fig. 19 shows Niyama results for the revised rigging simulation in the region that leaked with the original rigging. This figure emphasizes how much the minimum Niyama values in the region have risen compared to the original rigging (Fig. 17). In fact, the minimum Niyama value at the ID surface has risen to 3.0 (C-s)$^{1/2}$/mm, while the minimum value at the OD surface has risen to 4.7 (C-s)$^{1/2}$/mm. Again searching within a ± 5 mm (±0.20 in) neighborhood of the valve mid-plane, one finds that the OD surface minimum value is constant in this region, while the lowest ID surface value in this region is 2.9 (C-s)$^{1/2}$/mm. Since no leaks have occurred with the revised rigging, it can be concluded that micro-shrinkage sufficient to cause leaks does not exist at a Niyama value of 2.9 (C-s)$^{1/2}$/mm.

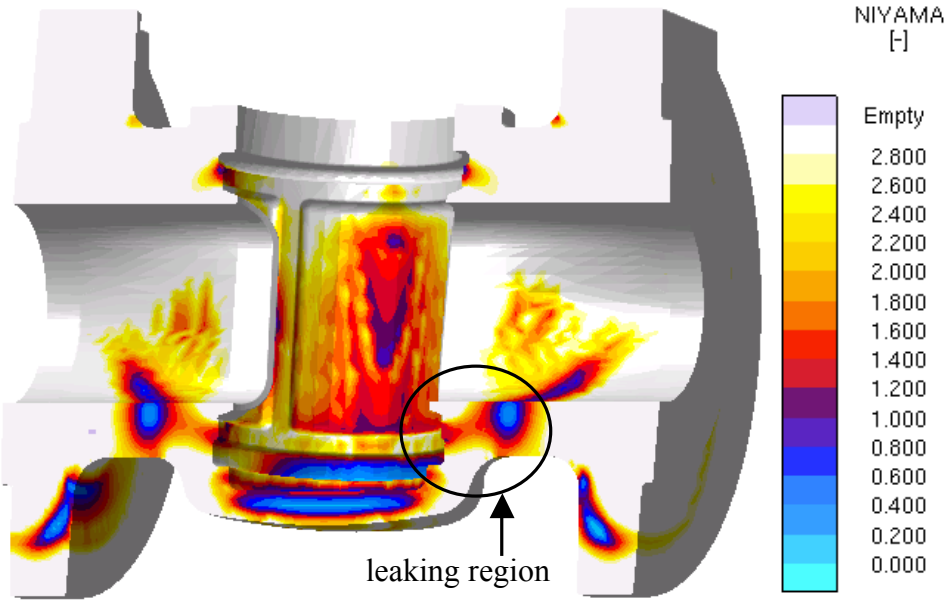

Fig. 16 Niyama criterion contours at the valve mid-plane for the simulation using the original rigging.

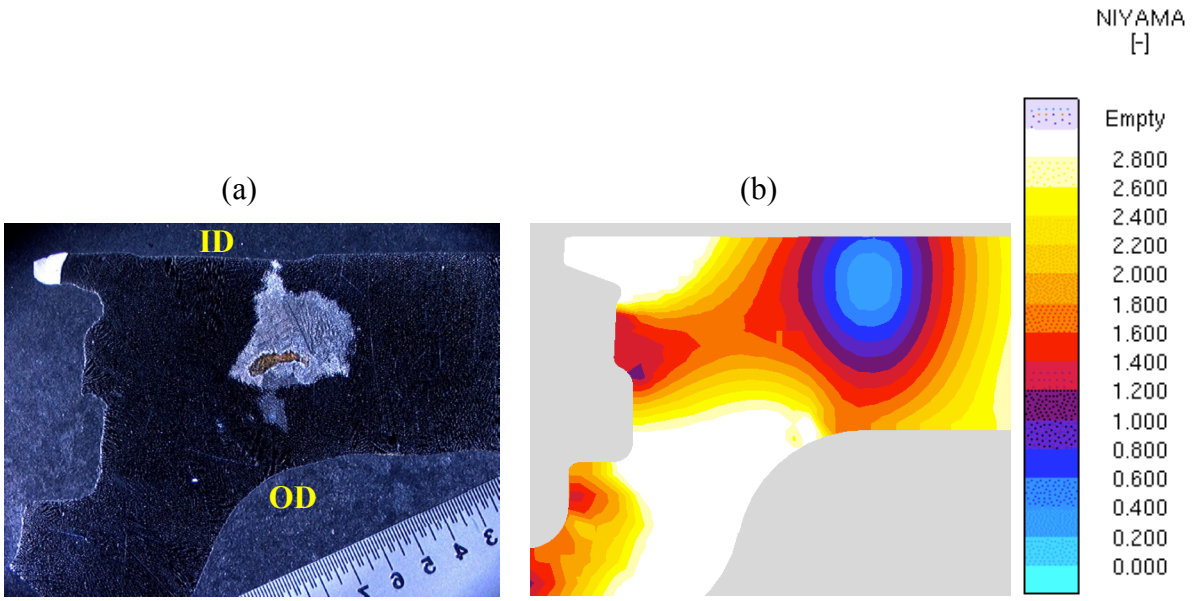

Fig. 17 Comparison between experiment and simulation results in the leaking region with the original rigging: (a) photograph of the cross-section of the leaking region (Fig. 15a, oriented to match simulation results); and (b) Niyama criterion contours at the valve mid-plane.

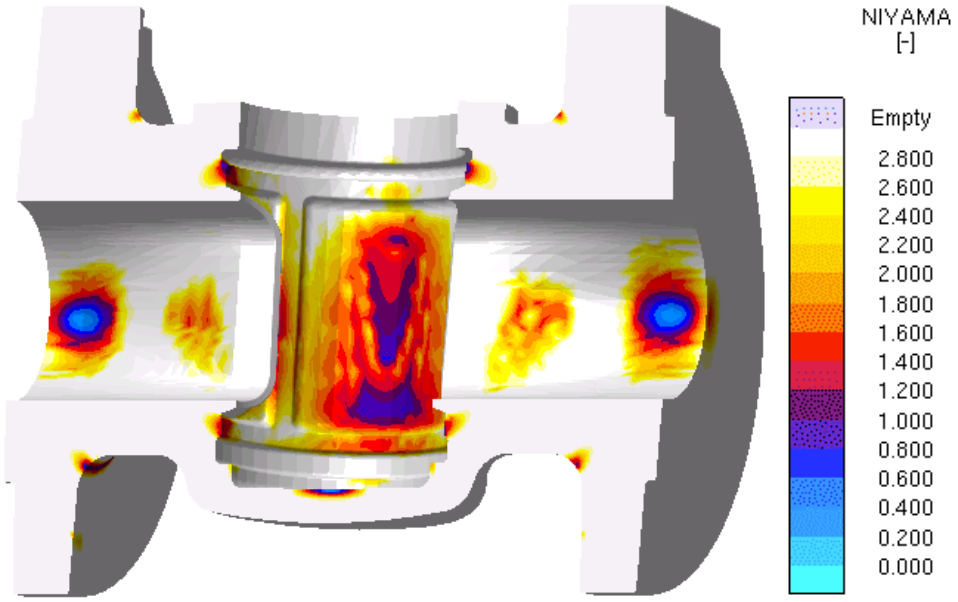

Fig. 18 Niyama criterion contours at the valve mid-plane for the simulation using the revised rigging.

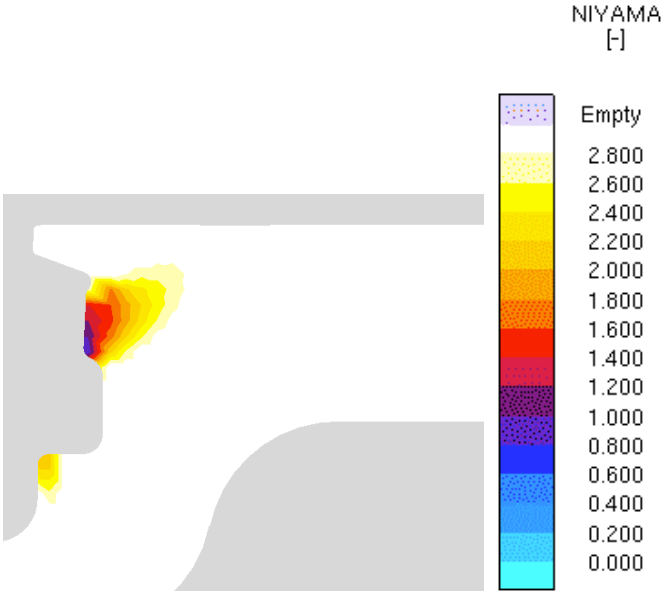

Fig. 19 Niyama criterion contours at the valve mid-plane in the original leaking region for the simulation using the revised rigging.

Conclusions

Previous research by the present authors[4] concluded that the Niyama criterion can be used to predict macro-shrinkage in high-nickel alloys (e.g., austenitic stainless steels and nickel-based alloys). The M35-1 and CN7M casting case studies presented here further corroborate the

predictive ability of the Niyama criterion to predict macro-shrinkage for these alloys. More importantly, these case studies also indicate that a correlation exists between the Niyama criterion and micro-shrinkage sufficient to cause leaks in high-nickel alloy castings. The comparisons between metallographic examination results and simulated Niyama values shown in this work indicate that macro-porosity may exist in regions with $Ny < Ny_{macro} = 1.0$ $(C\text{-}s)^{1/2}$/mm, which validates previous research[4]. These comparisons also indicate that noticeable amounts of micro-shrinkage may be present in casting regions with $Ny < Ny_{micro} = 2.0$ $(C\text{-}s)^{1/2}$/mm. These results imply that leaks in high-nickel alloy castings can be prevented by ensuring that simulated Niyama values are above 2.0 $(C\text{-}s)^{1/2}$/mm. This does not, however, imply that one should attempt to keep $Ny > 2.0$ $(C\text{-}s)^{1/2}$/mm throughout the casting. While that may be possible, it may be impractical and expensive to ensure such a high level of soundness throughout the casting. For the purpose of preventing leaks, it is only necessary to ensure that there not be a "pathway" of shrinkage porosity (micro- and/or macro-porosity) that leads from the inside to the outside of a fluid-containing casting.

Acknowledgements

The authors would like to thank the Materials Technology Institute (MTI), for their financial support of this research. We are also indebted to the Steel Founders' Society of America (SFSA) as well as to MTI, for their assistance in finding castings to use as case studies. The authors would also like to thank the customers who identified the case studies and provided the castings, as well as the foundries who provided the casting data necessary to perform the simulations. We would also like to express our gratitude to John Griffin of the University of Alabama at Birmingham, and to Willie Henderson of Honeywell, for providing us with photographs of the metallographic analyses of the case studies.

References

1. K.D. Carlson, S. Ou, R.A. Hardin, and C. Beckermann, "Development of New Feeding-Distance Rules Using Casting Simulation: Part I. Methodology," *Metall. Mater. Trans. B*, vol. 33B, pp. 731-740 (2002).
2. E. Niyama, T. Uchida, M. Morikawa, and S. Saito, "A Method of Shrinkage Prediction and its Application to Steel Casting Practice," *Am. Foundrymen's Soc. Int. Cast Met. J.*, vol. 7(3), pp. 52-63 (1982).
3. N. Jain, K.D. Carlson, and C. Beckermann, "Round Robin Study to Assess Variations in Casting Simulation Niyama Criterion Predictions," in Proceedings of the 61st Technical and Operating Conference, Steel Founders' Society of America, Chicago (2007).
4. K.D. Carlson, S. Ou, and C. Beckermann, "Feeding of High-Nickel Alloy Castings," *Metall. Mater. Trans. B*, vol. 36B, pp. 843-856 (2005).
5. MAGMASOFT v4.5, MAGMA GmbH, Aachen, Germany.
6. T. Midea and J.V. Shah, "Bringing Mold Material Thermophysical Data up to Speed," *Modern Casting*, vol. 94(8), pp. 30-33 (2004)